



Enantioselective Synthesis of Nonphosphorus-Containing Phosphotyrosyl Mimetics and Their Use in the Preparation of Tyrosine Phosphatase Inhibitory Peptides

Terrence R. Burke, Jr.,^{*,†} Zhu-Jun Yao,[‡] He Zhao,[‡]

George W. A. Milne,[‡] Li Wu,[§] Zhong-Yin Zhang[§] and Johannes H. Voigt[‡]

[†]*Laboratory of Medicinal Chemistry, Division of Basic Sciences*

National Cancer Institute, Bldg. 37, Rm. 5C06, National Institutes of Health, Bethesda, MD 20892 and

[§]*Department of Molecular Pharmacology, Albert Einstein College of Medicine, Bronx, NY 10461*

Received 13 March 1998; accepted 10 June 1998

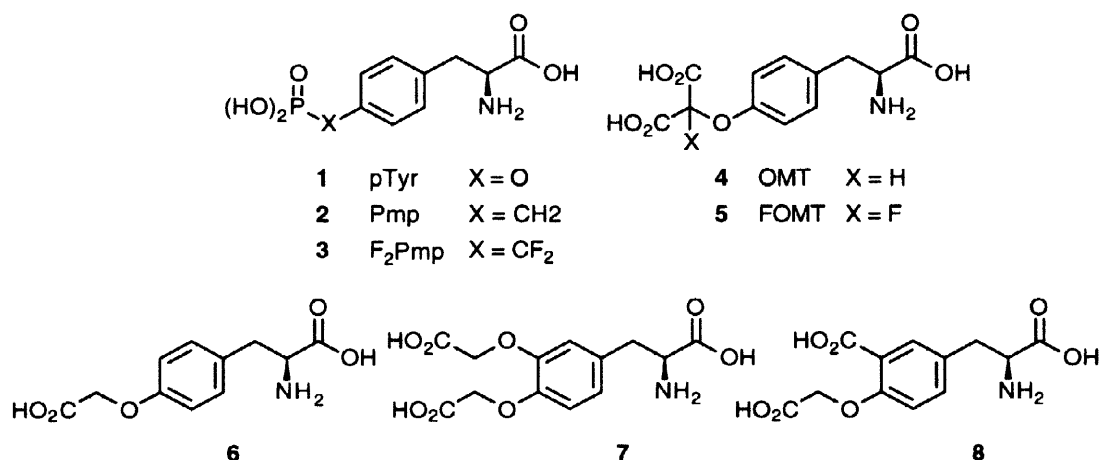
Abstract: Three new L-amino acid analogues **12**, **18** and **25** have been prepared in protected form suitable for incorporation into peptides by solid-phase synthesis using Fmoc protocols. These agents represent non-phosphorus-containing phosphotyrosyl (pTyr) mimetics, which utilize carboxylic groups to provide functionality normally afforded by the pTyr phosphate group. To demonstrate the utility of these analogues, the protein-tyrosine phosphatase-directed peptides Ac-D-A-D-E-X-L-amide (**28** - **30**) were prepared, where X = pTyr mimetic. In the case where X = 3-carboxy-4-(O-carboxymethyl)-L-tyrosine (**8**) a K_i value of 3.6 μM was obtained against PTP1, which equals the K_m of the parent pTyr containing peptide. Besides tyrosine phosphatases, these analogues may be useful in a number of contexts, including SH2 domain and phosphotyrosine binding domain systems. Published by Elsevier Science Ltd.

INTRODUCTION

The phosphotyrosyl (pTyr **1**) pharmacophore is a critical determinant in cellular signal transduction. Its inappropriate expression, either through generation by protein-tyrosine kinases (PTKs) or destruction by protein-tyrosine phosphatases (PTPs), can contribute to a variety of diseases, including immune disorders, cancers and diabetes. Therefore agents which modulate PTKs/PTPs are potentially useful as therapeutics, and considerable synthetic effort has been expended in the development of compounds which can mimic the pTyr pharmacophore in physiological systems.¹ Because in their natural environments, pTyr residues function as units of larger peptides or proteins, the focus of much research has been the preparation of pTyr-mimicking amino acid analogues suitably protected for peptide synthesis. Since it is the phosphate structure itself which imparts critical functionality to the tyrosyl residue, the development of phosphate mimetics which can be introduced onto phenylalanine platforms, has attracted the largest share of synthetic interest. While significant work has been reported in the development of phosphorous-based mimetics, such as phosphonomethyl phenylalanine (Pmp **2**)² and phosphonodifluoromethyl phenylalanine (F₂Pmp **3**),³ much less has been disclosed regarding non-phosphorus containing pTyr mimetics.

E-mail: tburke@helix.nih.gov

Among the most successful examples of non-phosphorus containing pTyr mimetics, are analogues that utilize the dicarboxylic acid-containing malonate structure as phosphate isosteres.⁴ These include *O*-malonyltyrosine (OMT 4)^{5,6} and fluoro-*O*-malonyltyrosine (FOMT 5),⁷ which in peptide contexts, are among the most potent PTP inhibitors yet reported.^{7,8} In an extension of our efforts to derive “carboxylate-based” pTyr mimetics, we have recently developed three new analogues, 6 - 8, which represent variants of the original malonate theme. Herein we report the synthesis of these new pTyr mimetics in protected form (compounds 12, 18 and 25, respectively) suitable for incorporation into peptides using Fmoc protocols. To demonstrate the potential utility of these agents, we have utilized them for the preparation of PTP-directed peptides and examine their interaction within the pTyr binding pocket using molecular dynamics (MD) simulations. Results of these simulations are then compared to actual K_i values obtained with the peptides.



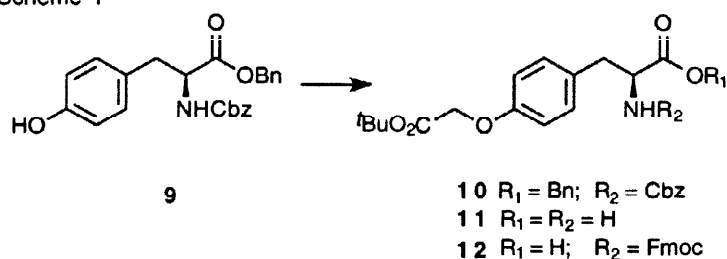
DESIGN RATIONALE

Many pTyr mimetics require highly charged phosphate-mimicking functionality for physiological potency. This charged character limits penetration through cell membranes, necessitating prodrug derivatization for cell-based studies. Carboxy-based pTyr mimetics such as OMT (4) were originally designed to potentially afford prodrug protection strategies which differed from those used for phosphorus-containing compounds. It was envisioned that the charged malonyl carboxyl groups could be masked in their ester forms, then liberated once inside cells to the free carboxyls via the action of cytoplasmic esterases.⁶ It was found however, that subjecting OMT diester-containing peptide to esterase treatment results in removal of only one ester,⁹ which is consistent with reports showing that only mono de-esterification of malonates occurs enzymatically.^{10,11} Since limitation to mono de-esterification could possibly result from close proximity of malonyl α,α -carboxyls, spatially separating the two carboxyls could potentially provide pTyr mimetics which are more amenable to enzyme mediated di de-esterification. For physiological potency as pTyr mimetics however, such “separated” dicarboxylics would also need to be in sufficiently close proximity as to display phosphate-mimicking character. Analogues 7 and 8 were therefore based on these considerations.

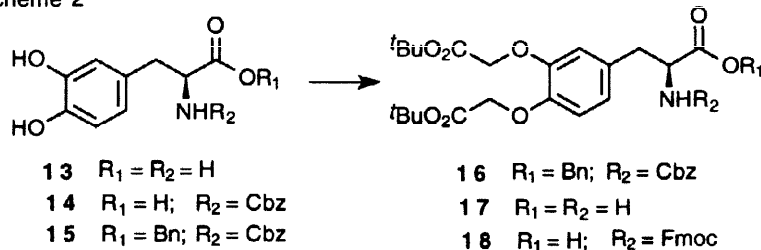
SYNTHETIC APPROACH

Amino Acid Analogues 12 and 18. The preparation of final products **12** and **18** started from tyrosine or dihydroxyphenylalanine respectively, and required initial selective protection of the amino and carboxylic acid groups in the presence of the free phenolic hydroxyls. Sequential derivatization of α -amino functionality as benzyloxycarbonyl (Cbz) derivatives was achieved using benzyl chloroformate, followed by esterification of carboxyls as benzyl (Bn) esters (cesium carbonate and benzyl bromide). Under these conditions, significant alkylation of the phenolic hydroxyls was not observed. Alkylation of free phenols as their *tert*-butyl carboxymethyl ethers was then achieved using *tert*-butyl α -bromoacetate under basic catalysis (NaH in DMF). For intermediates **10** and **16**, Cbz and Bn protecting groups were simultaneously removed by hydrogenolysis, with the resulting crude amino acids then being converted to final N-Fmoc-protected products **12** and **18** respectively, by treatment with 9-fluorenylmethyl-succinimidyl carbonate (Fmoc-Osu) (Schemes 1 and 2).

Scheme 1

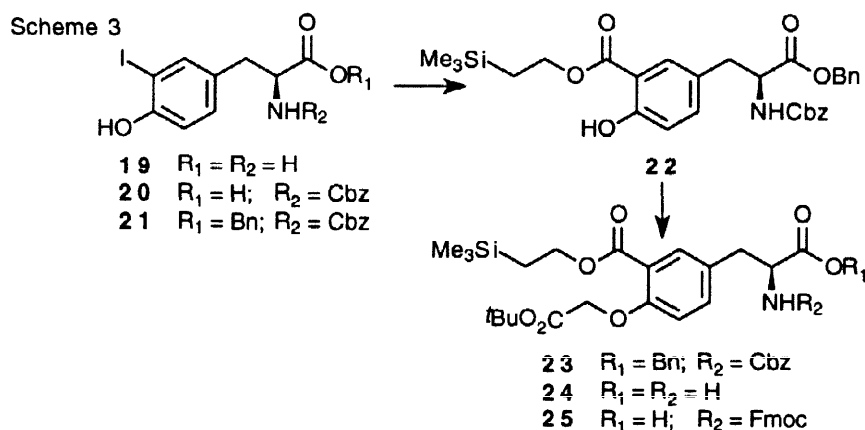


Scheme 2

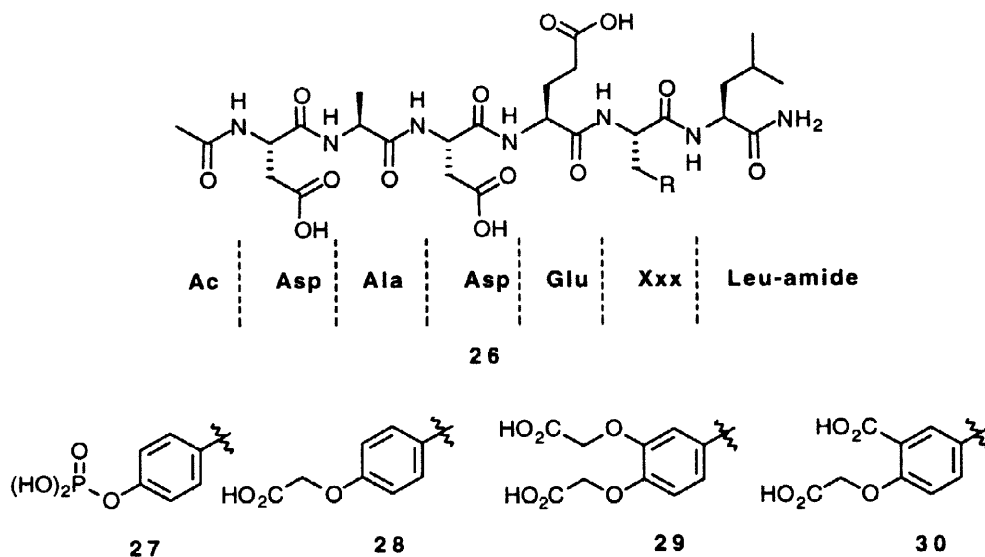


Amino Acid Analogue 25. Synthesis of 3'-carboxy-L-tyrosine analogue **8** in a form suitable for solid-phase synthesis was considerably more complex. Analogue **8** contains four functional groups which must be differentially protected. Unprotected **8** has previously been prepared in lengthy routes both as its racemate¹² and as its L-enantiomer.¹³ In the present situation however, the necessity for appropriate differential carboxyl protection of the final product makes these approaches unattractive. Synthetic routes towards L-DOPA derivatives which utilize 3-formyl¹⁴ and 3-acetyl¹⁵ substituted tyrosines could potentially afford avenues to differentially protected **8**, however in our hands such routes proved to be unfruitful. An alternate promising approach employing a fully elaborated 5-iodosalicylate for Pd-catalyzed coupling to iodoalanine¹⁶ also failed. As shown in Scheme 3, a fourth approach was therefore tried, in which the 3-carboxy functionality was introduced via Pd-catalyzed carbonylation using carbon monoxide. This route afforded a novel synthesis of the L-3-carboxytyrosine structure in which the resulting product (compound **25**) bears three distinct protecting groups that can be removed independently by treatment with base (Fmoc), acid (*tert*-butoxy) and fluoride ion (2-trimethylsilylethoxy).

Starting from commercially available 3'-iodo-L-tyrosine (**19**), conversion to the N - Cbz derivative **20** was achieved using benzyl chloroformate in an H₂O/dioxane/NaHCO₃ system. This is in contrast to a previous preparation of this compound using benzyl-8-chinolylcarbonate in DMF with NaOH.¹⁷ Following protection of the carboxylic acid as its benzyl ester **21**, conversion of the aryl iodide to the 3-((2-(trimethylsilyl)ethoxy)carbonyl) derivative **22** was accomplished by palladium-catalyzed carbonylation using carbon monoxide, 1,3-bis(diphenylphosphino)propane (DPP) and Pd(OAc)₂ in DMSO in the presence of triethylamine and 2-(trimethylsilyl)ethyl alcohol. The 4'-hydroxyl was then alkylated with *tert*-butyl α -bromoacetate (NaH in DMF) to give fully protected analogue **23**. Hydrogenolytic removal of Bn and Cbz groups gave crude amino acid **24**, which was converted to final product **25** prior to chromatographic purification (Scheme 3).



Peptide Synthesis. The peptide sequence Ac-Asp-Ala-Asp-Glu-Xxx-Leu-amide (**26**), (where Xxx = pTyr (**27**)), which corresponds to one of the cytoplasmic autophosphorylation sites of the epidermal growth factor receptor (EGFr₉₈₈₋₉₉₃), was originally shown to be a high affinity substrate for the rat PTP1 enzyme (K_m = 3.2 μ M).¹⁸ By replacing the pTyr residue in this sequence with non-hydrolyzable pTyr mimetics, we have previously demonstrated that high affinity PTP inhibitors can be obtained.^{7,8,19,20} In order to verify the utility of protected pTyr mimetics **12**, **18** and **25** in peptide synthesis, each was used in the solid-phase preparation of peptides modelled on sequence **26**. Fmoc protocols were utilized in combination with acid-labile Rink amide resin.²¹ Except for residue **25**, which contained 2-(trimethylsilyl)ethyl ester protection, *tert*-butyl protection of all side chain carboxylic functionality was removable by treatment with trifluoroacetic acid (TFA), which also resulted in peptide cleavage from the resin to provide final peptide products **28** and **29** directly. For peptide **30**, a deprotective cycle of tetrabutylammonium fluoride (TBAF) was employed to remove 2-(trimethylsilyl)ethyl ester protection prior to treatment with TFA. In solution synthesis, use of TBAF proves troublesome due to difficulties in removing tetrabutylammonium byproducts. In a solid-phase protocol however, all side products are washed from the resin prior to liberation of the peptide, obviating problems of tetrabutylammonium contamination. This makes the use of 2-(trimethylsilyl)ethyl ester protection quite attractive for solid-phase peptide synthesis. The successful synthesis of peptides **28** - **30** demonstrates the applicability of new pTyr mimetics **12**, **18** and **25** for peptide synthesis.



POTENTIAL APPLICATIONS

SH2 Domains. Phosphotyrosyl mimetics are of particular interest in the development of SH2 domain and PTP inhibitors. SH2 domains are highly homologous proteins in which binding of the pTyr phosphate involves critical interaction with two Arg residues. Figure 1 depicts one possible manner in which analogue **8** may afford key elements of this type of recognition. Although not shown in Figure 1, the ester oxygen linking the phosphate group to the tyrosine aryl ring contributes significantly to binding interactions. The analogue 4-(carboxymethyl)phenylalanine, which is a desoxy variant of compound **6**, has previously been prepared as a pTyr mimetic lacking such oxygen functionality.²² When examined as a pTyr mimetic in a Src SH2 domain binding system, 4-(carboxymethyl)phenylalanine showed extremely poor affinity.²³ Oxygen functionality linking carboxymethyl groups to aryl rings in **6** as well as **7** and **8**, could therefore enhance biological activity.

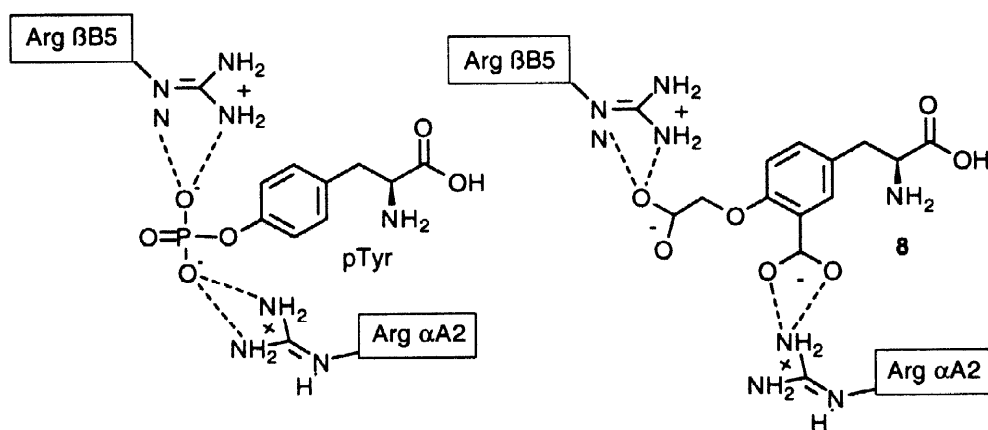


Figure 1. Schematic depiction of the interaction of the pTyr phosphate with two critical Arg residues in the Src SH2 domain (left),²⁴ and the manner in which the carboxyls of **8** could potentially afford similar features.

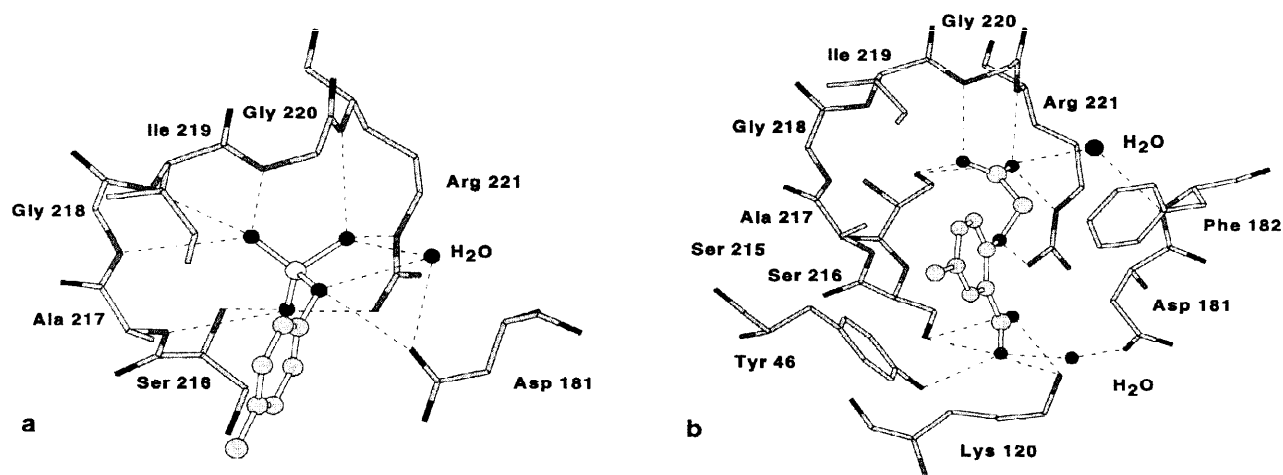


Figure 2. Orientation of ligand phenyl rings inside the PTP1B pTyr-pocket.²⁵ a) x-ray structure of **27**²⁶ b) modeled structure of **30**. The Graphic was generated using Quanta 97.²⁷

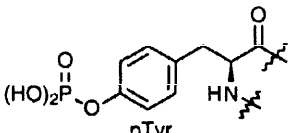
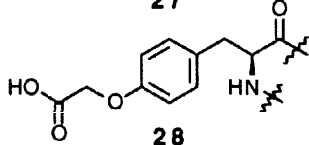
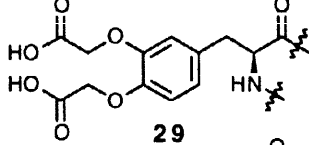
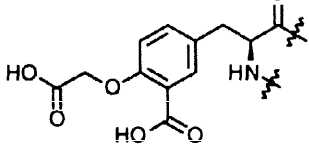
Protein-Tyrosine Phosphatases.

Molecular modelling.²⁵ Phosphotyrosyl mimetics have shown particular utility in the design of PTP antagonists, where greater latitude exists in structures exhibiting high binding affinity.²⁸ In the present study molecular modelling was undertaken to compare the PTP binding of pTyr mimetics with a parent pTyr residue. The crystal structure of “Asp-Ala-Asp-Glu-pTyr-Leu-NH₂” (**27**) bound to PTP1B²⁶ (Figure 2a) provided a starting structure for molecular modeling in which different binding modes to the phosphatase of pTyr and its analogues in peptides **27**, **29** and **30** were compared. To sample the conformational space of the complex sufficiently, 11 starting structures bound to PTP1B for **29** were generated and subjected to molecular dynamics simulation (MD), and 8 structures for **30** (see Experimental for details). For each MD simulation, the frame with the lowest energy was determined and these were compared to each other. For **30**, 5 out of the 8 structures displayed very similar phenyl ring orientations. The structure with the lowest energy is a member of this set of 5, and this structure was minimized (Figure 2b). In the case of peptide **29**, comparison of the lowest energy frames of the 11 MD runs did not show a uniform outcome. However the phenyl ring orientation in the structure with the lowest energy was similar to Figure 2b, and this was also minimized. The binding energy (E_b) can be expressed by the energy of the complex (E_c) and the energies of the free ligand (E_l^0) and the free receptor (E_r^0) (eq. (1)).²⁹ If one approximates E_l^0 by the gas phase energy of the ligand in the bound conformation (E_l), then one obtains ΔE_b for the energy difference between two ligands bound to the same receptor (eq. (2)). Entropy effects are neglected in these considerations. Applying eq. (2) to the minimized lowest energy frames for ligands **29** and **30** yielded a binding energy that was lower by 281.4 kcal/mol for **30** when compared to **29**.

$$(1) E_b = E_c - E_r^0 - E_l^0 \quad (2) \Delta E_b \approx (E_c^1 - E_l^1) - (E_c^2 - E_l^2)$$

K_i Determinations. To determine the utility of analogues **6**, **7** and **8** as PTP-directed pTyr mimetics, peptides **28** - **30** were examined against PTP1 catalyzed *p*-nitrophenyl phosphate (*p*NPP) hydrolysis at 30 °C and pH 7. The K_i values are summarized in Table 1. Mono-carboxy analogue **28** exhibited relatively poor binding affinity (K_i = 480 μM), while the di-carboxy compound **29** was approximately two-fold more potent (K_i = 199 μM). Peptide **30** showed significantly enhanced binding (K_i = 3.6 μM) relative to peptide **29**. The lower K_i value of **30** relative to **29** is consistent with molecular modelling predictions. The peptide **30** K_i value of 3.6 μM is equivalent to the K_m for the corresponding pTyr-containing peptide **27**, and is approximately three-fold better than the OMT-containing peptide against PTP1B (IC₅₀ = 10 μM).³⁰ Comparison of Figures 2a and 2b shows that, while for the pTyr-containing peptide **27**, the phosphate group binds to the pocket interacting with residues 216 to 221, in **30** only one carboxyl group binds to this pocket, interacting with residues 216, 220 and 221. The second carboxyl forms hydrogen bonds with Tyr 46, Lys 120, and Ser 216 and via a water molecule to Asp 181. This data potentially indicates highly favorable interaction of residue **8** within the PTP catalytic site. As such, the 3-carboxy-4-(O-carboxymethyl)phenyl moiety found in **8** may be useful as a phenylphosphate isostere for the further design of PTP antagonists.

Table 1. Kinetic constants measured against PTP1 preparations for the peptides "Ac-D-A-D-E-X-L-amide"

X	K _i (or K _m) ± s.d. μM
 <p>pTyr 27</p>	3.2 ± 0.5 ^a
 <p>28</p>	480 ± 20
 <p>29</p>	199 ± 13
 <p>30</p>	3.6 ± 0.2

^aPreviously reported.¹⁸

CONCLUSION

Three novel, non-phosphorus containing pTyr mimetics have been described in forms suitable for solid-phase synthesis. These agents may be useful in a variety pTyr-dependent cell signalling contexts, including the preparation of inhibitors directed against protein-tyrosine binding domains, SH2 domains and PTPs.

EXPERIMENTAL

Molecular modelling.²⁵ All simulations were performed with the Insight II 97.0/Discover 3.0 modeling package²⁷ using the cff91-force field. The charge of the phenylether oxygen in **29** and **30** was calculated with Spartan³¹ 4.04 using the STO-3G basis set. The crystal structure of **27** bound to PTP1B was used as the starting geometry. Compound **27** in the bound conformation was taken out of the receptor modified appropriately to yield **29** and **30**. A quenched molecular dynamics simulation (NVT ensemble) of 80 ps at 1000 K was performed. Every 100 fs the coordinates of the structure were saved and then minimized by 300 steps of the Polak-Ribiere conjugated gradient algorithm (CG-PR). Everything but the side chain of the pTyr mimetic residue was fixed during the simulation. The resulting 800 structures for each peptide were grouped into 11 clusters with a cutoff of 0.8 Å² for **29**, and 8 clusters with a cutoff of 0.5 Å² for **30**. A representative structure of each cluster was modeled into the PTP1B binding pocket by superimposing the backbone atoms of **29** or **30** with those of the pTyr-containing **27** in the crystal structure. The resulting 11 structures for **29** and 8 structures for **30** were then solvated with a 20 Å sphere of 714 water molecules centered around Cα of Glu 4 of the hexapeptide. All structures were minimized with 300 steps of CG-PR and subjected to 20 ps MD at 398 K, 20 ps at 348 K and 50 ps at 298 K in an NVT ensemble. During minimization and simulation, all atoms were held fixed except the hexapeptide, the water molecules in a sphere of radius 14 Å around the Cα of Glu 4 and the side chains of PTP1B within 6 Å around the initial conformation of the hexapeptides. For the last 50 ps of the MD the coordinates were saved every 1.0 ps. The frames with the lowest energy for each of the 11 and 8 runs for **29** and **30** respectively, were determined. For **29** the lowest energy structure out of the 11 frames was minimized with 19 steps of steepest decent (SD) and 500 steps of CG-PG. For **30** the lowest energy structure out of the 8 frames was minimized with 24 steps SD and 500 steps of CG-PR. During final energy minimizations, all constraints were released. A constant dielectric constant of 1.00 and the cell multipole method with the fine accuracy for all nonbonding interactions was used.

Determination of K_i values. Recombinant PTP1 was expressed and purified as described.³² Inhibition constants for **27** - **30** were determined for homogeneous PTP1 in the following manner. At various fixed concentrations of inhibitors (0, 100, and 300 μM), the initial rate at eight different *p*-nitrophenyl phosphate concentrations (0.2 Km to 5 Km) was measured as described.³³ The data were fit to the equation “ $v = V_{\max} \cdot S / (K_m \cdot [1 + K_i] + S)$ ” using KINETASYST (IntelliKinetics, State College, PA) to obtain inhibition constants (K_i values).

Synthetic. Melting points were determined on a Mel Temp II melting apparatus and are uncorrected. Elemental analysis were obtained from Atlantic Microlab Inc., Norcross, GA. and amino acid analysis were obtained from Peptide Technologies Corporation, Gaithersburg, MD. Fast atom bombardment mass spectra (FABMS) were acquired with a VG Analytical 7070E mass spectrometer under the control of a VG 2035 data system. ¹H NMR data were obtained on Bruker AC250 (250 MHz) instrument. Removal of solvents was performed by rotary evaporation under reduced pressure.

(L)-N-Cbz-4-(((tert-butyl)oxycarbonyl)methoxy)-phenylalanine benzyl ester (10). Into a suspension of NaH (60 % dispersion in mineral oil, 4 g (10 mmol)) in anhydrous DMF (40 mL) under argon, was added a solution of *N*^α-Cbz-L-tyrosine benzyl ester (**9**)³⁴ (4.05 g, 10 mmol) in anhydrous DMF (40 mL) dropwise over 10 minutes at room temperature. After stirring for 30 minutes, *tert*-butyl α-bromoacetate (4.43 mL, 30 mmol) was added dropwise over 10 minutes, then the mixture was stirred (overnight). Solvent was removed and residue was diluted with EtOAc, washed with brine, dried over anhydrous Na₂SO₄, and taken to dryness. Purification by silica gel chromatography (EtOAc : hexane = 1 : 4) and crystallization (ether-hexane) provide **10** as a white solid (4.7 g, 90%): mp 87-88 °C (ether-hexane); ¹H NMR (CDCl₃) δ 7.33-7.24 (m, 10H), 6.88 (d, *J* = 8.4 Hz, 2H), 6.7 (d, *J* = 8.5 Hz, 2H), 5.18-4.99 (m, 4H), 4.64 (m, 1H), 4.44 (s, 2H), 3.03 (d, *J* = 5.5 Hz, 2H), 1.46 (s, 9H). Calcd. for C₃₀H₃₃NO₇: C, 69.35; H, 6.40; N, 2.70. Found: C, 69.48; H, 6.47; N, 2.64.

(L)-4-(((tert-butyl)oxycarbonyl)methoxy)-phenylalanine (11). A solution of **10** (1 g, 1.9 mmol) in MeOH (50 mL) was hydrogenated over 10% Pd•C (100 mg) under 40 psi of hydrogen in a Parr apparatus (room temperature, overnight). The reaction mixture was filtered through celite, concentrated, and crystallized from MeOH-hexane to provide **11** (510 mg, 91%) as a white solid: mp 181-185 °C (MeOH-hexane); ¹H NMR (DMSO-*d*₆) δ 7.16 (d, *J* = 8.5 Hz, 2H), 6.99 (d, *J* = 8.5 Hz, 2H), 4.58 (s, 2H), 3.34 (d, *J* = 4.3 Hz, 1H), 3.31 (d, *J* = 4.3 Hz, 1H), 3.05 (dd, *J* = 14.3, 4.2 Hz, 1H), 2.79 (d, *J* = 14.3 Hz, 1H), 2.76 (d, *J* = 14.3 Hz, 1H), 1.43 (s, 9H). Calcd. for C₁₅H₂₁NO₅•1/4H₂O: C, 60.09; H, 7.23; N, 4.67. Found: C, 60.04; H, 7.04; N, 4.83.

(L)-N-Fmoc-4-(((tert-butyl)oxycarbonyl)methoxy)-phenylalanine (12). A mixture of **11** (1.5 g, 5 mmol), Fmoc-OSu (1.69 g, 5 mmol) and KHCO₃ (2 g, 25 mmol) in dioxane (20 mL) and water (20 mL) was stirred at room temperature (overnight). After adjusting the reaction mixture to pH ~ 2 by addition of 3N HCl, dioxane was removed by rotary evaporation. Residue was taken up in EtOAc (500 mL), washed with brine, dried over anhydrous Na₂SO₄ and taken to dryness. Purification by silica gel chromatography (CHCl₃ : MeOH = 1 : 3) and crystallization (CHCl₃-hexane) provided **12** as a white solid (2.25 g, 87%): mp 194-197 °C (MeOH-hexane); ¹H NMR (DMSO) δ 7.88 (d, *J* = 7.3 Hz, 2H), 7.63 (d, *J* = 7.2 Hz, 2H), 7.64-7.32 (m, 4H), 7.06 (d, *J* = 8.2 Hz, 2H), 6.69 (d, *J* = 8.3 Hz, 2H), 4.51 (s, 2H), 4.33-4.27 (m, 1H), 4.18-4.06 (m, 2H), 3.89 (m, 1H), 3.04 (dd, *J* = 14.3, 4.0 Hz, 1H), 2.85 (m, 1H), 1.39 (s, 9H). FABMS *m/z* 516 (M-H). Calcd. for C₃₀H₃₁NO₇•1C₄H₈O₂: C, 67.91; H, 6.39; N, 2.40. Found: C, 67.93; H, 6.74; N, 2.23. HR-FABMS (MH⁺) calcd for C₃₀H₃₁NO₇: 516.2022; Found: 516.2020.

(L)-N-Cbz-3,4-dihydroxyphenylalanine benzyl ester (15). To a suspension L-3,4-dihydroxyphenylalanine (**13**) (1.97 g; 10 mmol) and NaHCO₃ (8.40 g; 100 mmol) in H₂O (50 mL) with dioxane (50 mL) was added benzyl chloroformate (1.43 mL; 10 mmol) and the reaction stirred at room temperature under argon (overnight). The mixture was partitioned between 1 N HCl/brine and EtOAc (300 mL); dried (MgSO₄) and taken to dryness, yielding L-*N*^α-benzyloxycarbonyl-3,4-dihydroxyphenylalanine (**14**) as a syrup. This was dissolved in H₂O (30 mL) and DMF (30 mL) containing CsCO₃ (1.63 g; 5 mmol), then taken to dryness under high vacuum. The residue in anhydrous DMF (30 mL) was stirred with benzyl bromide (1.19 mL; 10 mmol) at

room temperature under argon (overnight). The reaction mixture was partitioned between saturated aqueous NaHCO_3 /brine (300 mL) and CHCl_3 (2 x 100 mL); washed with 1 N HCl/brine (100 mL); dried (MgSO_4) and taken to dryness, yielding a syrup (4.19 g). Purification by silica gel chromatography was accomplished using EtOAc in hexanes: From 0% to 20% EtOAc eluted impurity, with 50% EtOAc eluting product **15** as a syrup (2.54 g; 60% yield). ^1H NMR (CDCl_3) δ 7.34 (10H, m), 6.68 (d, $J = 8.1$ Hz, 1H), 6.39 (m, 2H), 5.10~5.40 (m 5H), 4.64 (m, 1H), 2.97 (m, 2H), 2.08~2.67 (br, 2H).

(L)-N-Cbz-3,4-di(((tert-butyl)oxycarbonyl)methoxy)-phenylalanine benzyl ester (16). A mixture **15** (2.54 g; 6.0) and *tert*-butyl α -bromoacetate (2.14 mL; 14.5 mmol) in anhydrous DMF (30 mL) with powdered K_2CO_3 (1.99 g; 14.5 mmol) was stirred at room temperature under argon (overnight). The resulting fine white suspension was partitioned between brine (200 mL) and EtOAc (2 x 100 mL); washed with brine (2 x 100 mL); dried (MgSO_4) and taken to dryness, yielding a syrup (3.77 g). Purification by silica gel chromatography (20% EtOAc in hexanes provided product **16** as a colorless syrup (3.15 g; 81% yield): ^1H NMR (CDCl_3) δ 7.41 (m, 10H), 6.77 (d, $J = 7.7$ Hz, 1H), 6.67 (m, 2H), 5.22 (m, 5H), 4.70 (m, 1H), 4.63 (s, 2H), 4.55 (s, 2H), 3.10 (d, $J = 6.0$ Hz, 2H), 1.55 (s, 9H), 1.54 (9H, s). Calcd. For $\text{C}_{36}\text{H}_{43}\text{NO}_{10}$: C, 66.55; H, 6.67; N, 2.16. Found: C, 66.50; H, 6.73; N, 2.19. FABMS (+VE, NBA) m/z : 649 (MH^+).

(L)-3,4-di(((tert-Butyl)oxycarbonyl)methoxy)-phenylalanine (17). A solution of **16** (3.00 g; 4.6 mmol) in MeOH (75 mL) was shaken in a Parr apparatus under 40 psi H_2 over palladium black (100 mg) for 24 h, then collected by filtration and taken to dryness, yielding **17** as a white foam (1.67 g; 85%): ^1H NMR (DMSO) δ 6.88 (s, 1H), 6.83 (s, 2H), 4.67 (s, 2H), 4.65 (s, 2H), 3.41 (NH_2 and $-\text{CHN}-$, overlapped by H_2O 3H), 3.10 (dd, $J = 3.4\text{Hz}$, 14.1Hz , 1H), 2.76 (dd, $J = 8.6\text{Hz}$, 14.6 Hz, 1H), 1.49 (s, 18H); ($-\text{COOH}$ was not detected). Calcd. For $\text{C}_{21}\text{H}_{31}\text{NO}_8$: C, 59.28; H, 7.34; N, 3.29. Found: C, 59.05; H, 7.31; N, 3.25. FABMS (+VE, NBA) m/z : 426 (MH^+).

(L)-N-Fmoc-3,4-di(((tert-butyl)oxycarbonyl)methoxy)-phenylalanine (18). A mixture of **17** (829 mg; 2.0 mmol), NaHCO_3 (840 mg; 10 mmol) and Fmoc-OSu (657 mmol; 2.0 mmol) in H_2O (10 mmol) and dioxane (10 mL) was stirred at room temperature (overnight), then partitioned between ice-cold 0.2 N HCl/brine (300 mL) and EtOAc (2 x 100 mL); dried (MgSO_4) and taken to dryness, yielding a foam (1.34 g). Purification by silica gel chromatography was initially performed using EtOAc in hexanes from 0% to 50% EtOAc. A second purification was then undertaken using from 0% to 30% EtOAc in hexanes to provide **18** as a white foam (878 mg; 68%); ^1H NMR (CDCl_3) δ 7.83 (d, $J = 7.7$ Hz, 2H), 7.63 (m, (2H), 7.42 (m, 4H), 6.82 (m, 3H), 5.50 (d, $J = 8.2\text{Hz}$, 1H), 4.73 (m, 1H), 4.63 (s, 4H), 4.45 (d, $J = 6.8$ Hz, 2H), 4.27 (m, 1H), 3.14 (m, 2H), 1.55 (s, 9H), 1.54 (s, 9H); ($-\text{COOH}$ was not detected). Calcd. For $\text{C}_{36}\text{H}_{41}\text{NO}_{10}$: C, 66.76; H, 6.38; N, 2.16. Found: C, 66.53; H, 6.57; N, 2.07. FABMS (-VE, NBA) m/z : 646 (M-H).

(L)-N-Cbz-3-iodotyrosine benzyl ester (21). To a suspension of 3-iodotyrosine (**19**) (1.0 g, 3.26 mmol) and NaHCO₃ (2.74 g; 32.6 mmol) in H₂O (15 mL) with dioxane (15 mL) was added dropwise, benzyl chloroformate (466 μ L; 3.26 mmol) in dioxane (5 mL) and the reaction stirred at room temperature (5 h). The mixture was partitioned between 1 N HCl (100 mL) and EtOAc (2 x 50 mL); dried (MgSO₄) and taken to dryness, yielding (L)-N-Cbz-3-iodotyrosine (**20**) as a resin. This was dissolved with slight warming in H₂O (20 mL) containing CsCO₃ (1.06 g; 3.26 mmol), then taken to dryness under high vacuum. The residue in anhydrous DMF (20 mL) was stirred with benzyl bromide (388 μ L; 3.26 mmol) at room temperature under argon (overnight). The reaction mixture was partitioned between saturated aqueous NaHCO₃/brine (100 mL) and EtOAc (2 x 100 mL); washed with aqueous NaHCO₃/brine (2 x 100 mL); dried (MgSO₄) and taken to dryness, yielding an oil (1.64 g). Purification by silica gel chromatography was accomplished using EtOAc in hexanes, from 0% to 20% EtOAc, yielding **21** as a snow-white solid (566 mg; 33% yield): ¹H NMR (CDCl₃) δ 7.43 (m, 11H), 6.94 (d, J = 8.1 Hz, 1H), 6.85 (d, J = 8.5 Hz, 1H), 5.52 (brs, 1H), 5.37 (d, J = 8.1 Hz, 1), 5.19 (m, 4H), 4.72 (m, 1H), 3.08 (m 2H). Calcd. For C₂₄H₂₂NO₅I: C, 54.25; H, 4.17; N, 2.64. Found: C, 54.71; H, 4.26; N, 2.55. FABMS (+VE, NBA) m/z : 532 (MH⁺).

(L)-N-Cbz-3-((2-(trimethylsilyl)ethoxy)carbonyl)-tyrosine benzyl ester (22). A mixture of **21** (2.66 g; 5.0 mmol), Pd(OAc)₂ (112 mg; 0.5 mmol) and di(diphenylphosphoryl)propane (DPP) (206 mg; 0.5 mmol) was placed in a rb which was evacuated then charged with CO gas. To this was added a solution of 2-trimethylsilylethanol (1.77 mL; 15 mmol) and triethylamine (2.60 mL; 15 mmol) in anhydrous DMSO (5.6 mL), and the mixture stirred at 75° C (overnight). After cooling to room temperature, the mixture was partitioned between 1 N HCl/brine (200 mL) and EtOAc (2 x 100 mL); washed with 1 N HCl/brine (2 x 100 mL); dried (MgSO₄) and taken to dryness, yielding a thick, dark brown syrup (3.83 g). Purification by silica gel chromatography was accomplished using EtOAc in hexanes, from 0% to 30% EtOAc, yielding **22** as a white solid (1.11 g; 49% yield; 71% yield based on 1.15 g recovered starting **21**): ¹H NMR (CDCl₃) δ 10.08 (s, 1H), 7.58 (s, 1H), 7.34 (m, 10H), 7.08 (dd, J = 8.2 Hz, 1.7 Hz, 1H), 6.82 (d, J = 8.6 Hz, 1H), 5.24 (d, J = 7.7 Hz, 1H), 5.14 (s, 2H), 5.10 (s, 2H), 4.67 (m, 1H), 4.40 (t, J = 8.6 Hz, 2H), 3.04 (m, 2H), 1.10 (t, J = 8.6 Hz, 2H), 0.08 (s, 9H). Calcd. For C₃₀H₃₅NO₇Si: C, 65.55; H, 6.42; N, 2.55. Found: C, 65.48; H, 6.53; N, 2.46. FABMS (+VE, NBA) m/z : 550 (MH⁺).

(L)-N-Cbz-4-(((tert-butyl)oxycarbonyl)methyl)-3-((2-(trimethylsilyl)ethoxy)carbonyl)-tyrosine benzyl ester (23). A mixture of **22** (164 mg; 0.29 mmol), *tert*-butyl α -bromoacetate (51 μ L; 0.35 mmol) and powdered K₂CO₃ (48 mg; 0.35 mmol) in anhydrous DMF (1 mL) was stirred at room temperature (overnight). The resulting fine white suspension was partitioned between brine (50 mL) and EtOAc (2 x 50 mL); dried (MgSO₄) and taken to dryness, to provide **23** as a syrup (180 mg; 97% yield): ¹H NMR (CDCl₃) δ 7.64 (s, 1H), 7.42 (m, 10H), 7.14 (d, J = 8.2 Hz, 1H), 6.76 (d, J = 8.5 Hz, 1H), 5.31 (d, J = 7.7 Hz, 1H), 5.21 (s, 2H), 5.17 (s, 2H), 4.73 (m, 1H), 4.63 (s, 2H), 4.44 (t, J = 8.5 Hz, 2H), 3.15 (m, 2H), 1.55 (s, 9H), 1.18 (t, J =

8.6 Hz, 2H), 0.14 (s, 9H). Calcd. For $C_{36}H_{45}NO_9Si$: C, 65.14; H, 6.83; N, 2.11. Found: C, 64.92; H, 6.90; N, 2.25. FABMS (+VE, NBA) m/z : 664 (MH⁺).

(L)-4-(((tert-Butyl)oxycarbonyl)methyl)-3-((2-(trimethylsilyl)ethoxy)carbonyl)-tyrosine (24). A solution of **23** (1.21 g; 1.82 mmol) in MeOH (75 mL) was shaken in a Parr apparatus under 40 psi H_2 over palladium black (250 mg) (overnight), then collected by filtration and taken to dryness, yielding **24** as a glass (694 mg; 87%): 1H NMR (DMSO) δ 7.50 (s, 1H), 7.36 (d, J = 8.5 Hz, 1H), 6.88 (, J = 8.5 Hz, 1H), 4.63 (s, 2H), 4.27 (t, J = 8.3 Hz, 2H), 3.70 (NH₂, overlapped by water, 2H), 3.46 (-CHN-, m, 1H), 3.07 (dd, J = 4.3 Hz, 14.6 Hz, 1H), 2.84 (dd, J = 7.7 Hz, 14.1 Hz, 1H), 1.40 (s, 9H), 1.04 (t, J = 8.5 Hz, 2H), 0.03 (s, 9H); (-COOH did not show). Calcd. For $C_{21}H_{33}NO_7Si$: C, 56.23; H, 7.64; N, 3.12. Found: C, 56.51; H, 7.51; N, 3.02. FABMS (-VE, NBA) m/z : 438 (M-H).

(L)-N-Fmoc-4-(((tert-butyl)oxycarbonyl)methyl)-3-((2-(trimethylsilyl)ethoxy)carbonyl)-tyrosine (25). A mixture of **24** 409 mg; 0.93 mmol), NaHCO₃ (390 mg; 4.65 mmol) and Fmoc-OSu (313 mg; 0.93 mmol) in H₂O (10 mmol) and dioxane (10 mL) was stirred at room temperature (overnight), then partitioned between ice-cold 0.2 N HCl/brine (100 mL) and EtOAc (2 x 100 mL); dried (MgSO₄) and taken to dryness, yielding a syrup (644 mg). Purification by silica gel chromatography using EtOAc in hexanes from 0% to 50% EtOAc provided **25** as a syrup (547 mg; 89%); 1H NMR (CDCl₃) δ 7.84 (d, J = 7.7 Hz, 2H), 7.71 (s, 1H), 7.63 (m, 2H), 7.43 (m, 4H), 7.28 (d, J = 8.1 Hz, 1H), 6.84 (d, J = 8.5 Hz, 1H), 5.39 (d, J = 8.1 Hz, 1H), 4.73 (m, 1H), 4.64 (s, 2H), 4.44 (m, 4H), 4.28 (m, 1H), 3.22 (m, 2H), 1.55 (s, 9H), 1.17 (t, J = 7.3 Hz, 2H), 0.12 (s, 9H); (-COOH did not show). Calcd. For $C_{36}H_{43}NO_9Si \cdot 1\frac{3}{4}H_2O$: C, 62.36; H, 6.76; N, 2.02. Found: C, 62.03; H, 6.36; N, 1.99. FABMS (-VE, NBA) m/z : 660 (M-H).

Solid-phase synthesis of peptides 28 - 30. Synthesis of peptides was achieved using manual solid-phase techniques. In a representative procedure, a total of 0.2 milliequivalents of N-Fmoc Rink amide resin (Bachem, 0.46 milliequivalents/g) was washed well with several 2 mL portions of N-methyl-2-pyrrolidone (NMP), then the Fmoc amino protection was removed by treatment with 20% piperidine in NMP (2 mL, 20 minutes). The deblocked resin was washed well with NMP (10 x 2 mL) then coupled overnight with a solution of active ester formed by reacting 0.5 mmol each of N-Fmoc-L-Leu, 1-hydroxybenzotriazole (HOBT) and 1,3-diisopropylcarbodiimide (DIPCDI) in NMP (2 mL, 10 minutes). The resin was washed with NMP (10 x 2 mL), and the amino Fmoc-protection was removed by treatment with 20% piperidine in NMP (2 mL; 20 minutes). Subsequent residues were attached in an similar fashion using HOBT ester preactivation, followed by Fmoc cleavage. Order of addition was pTyr mimicking analogues (**12**, **18** or **25**); Fmoc-Glu(^tBu)-OH; Fmoc-Asp(^tBu)-OH; Fmoc-Ala-OH; Fmoc-Asp(^tBu)-OH. The completed N-terminally deprotected resins were acetylated using N-acetyl imidazole (110 mg, 1 mmol, overnight) in NMP (1 mL). Peptides were cleaved from the resins using a mixture of TFA (1.85 mL), H₂O (100 μ L) and triethylsilane (50 μ L) (1 h). In the case of peptide **30**, the (2-(trimethylsilyl)ethoxy) protecting group was removed prior to peptide cleavage from the resin, by treatment with tetrabutylammonium fluoride, 1.0 M in THF (10 equivalents) in NMP (2 h). Crude peptides were purified by

HPLC using a Vydac Peptide and Protein C₁₈ reverse phase column with a binary solvent system of 0.1% TFA in H₂O and 0.1% TFA in acetonitrile.

Peptide 28: (85% yield): FABMS (–VE, Gly) m/z 822 (M-H). Calcd. for C₃₅H₄₉N₇O₁₆•3H₂O: C, 47.89; H, 6.32; N, 11.17. Found: C, 47.66; H, 5.89; N, 10.85. Amino acid analysis: Asp 2.00 (2), Glu 1.06 (1), Ala 0.99 (1), Leu 1.01 (1).

Peptide 29: (50% yield): ¹H NMR (D₂O) δ 6.89–7.05 (m, 3H), 4.83 (s, part of it was overlapped by water peak, 4H), 4.69 (m, 3H), 4.30 (m, 3H), 3.17 (m, 1H), 2.93 (m, 5H), 2.31 (t, $J = 7.3$ Hz, 2H), 2.08 (s, 3H), 1.96 (m, 2H), 1.62 (s, 3H), 1.44 (d, $J = 7.3$ Hz, 3H), 0.95 (d, $J = 5.4$ Hz, 3H), 0.88 (d, $J = 5.4$ Hz, 3H). Calcd. For C₃₇H₅₁N₇O₁₉•¹/₂H₂O•¹/₂CF₃CO₂H: C, 47.35; H, 5.49; N, 10.17. Found: C, 47.10; H, 5.29; N, 9.95. FABMS (–VE, Gly) m/z 896 (M-H). Amino acid analysis: Asp 2.15 (2), Glu 1.07 (1), Ala 0.90 (1), Leu 1.00 (1).

Peptide 30: (35% yield): ¹H NMR (D₂O) δ 7.76 (s, 1H,), 7.50 (d, $J = 8.3$ Hz, 1H), 7.07 (d, $J = 8.5$ Hz, 1H), 4.84 (s, overlapped by water, 2H), 4.75 (m, 2H), 4.64 (m, 1H), 4.30 (m, 3H), 2.99–3.25 (m, 2H), 2.84 (m, 4H), 2.29 (m, 2H), 2.02 (s, 3H), 1.90 (m, 2H), 1.58 (s, 3H), 1.39 (d, $J = 6.6$ Hz, 3H), 0.92 (d, $J = 3.8$ Hz, 3H), 0.85 (d, $J = 3.7$ Hz, 3H). Calcd. For C₃₆H₄₉N₇O₁₈•H₂O•³/₄CF₃CO₂H: C, 46.37; H, 5.37; N, 10.09. Found: C, 46.30; H, 5.20; N, 9.81. FABMS (–VE, Gly) m/z 866 (M-H). Amino acid analysis: Asp 2.08 (2), Glu 1.05 (1), Ala 0.90 (1), Leu 1.00 (1).

Acknowledgments. Appreciation is expressed to Ms. Pamela Russ and Dr. James Kelley of the LMC and to Dr. Noel Whittaker of the NIDDK for mass spectral analysis. L.W. and Z.-Y. Z. were supported in part by a National Institutes of Health Grant CA69202 and by a Pilot Research Grant from the Cancer Center of Albert Einstein College of Medicine.

REFERENCES

1. Burke, T. R., Jr.; Yao, Z.-J.; Smyth, M. S.; Ye, B. *Current Pharmaceutical Design* **1997**, *3*, 291-304.
2. Marseigne, I.; Roques, B. P. *J. Org. Chem.* **1988**, *53*, 3621-3624.
3. Burke, T. R., Jr.; Smyth, M.; Nomizu, M.; Otaka, A.; Roller, P. P. *J. Org. Chem.* **1993**, *58*, 1336-1340.
4. Miller, M. J.; Braccolino, D. S.; Cleary, D. G.; Ream, J. E.; Walker, M. C.; Sikorski, J. A. *Bioorg. Med. Chem. Lett.* **1994**, *4*, 2605-2608.
5. Kole, H. K.; Ye, B.; Akamatsu, M.; Yan, X.; Barford, D.; Roller, P. P.; Burke, T. R., Jr. *Biochem. Biophys. Res. Commun.* **1995**, *209*, 817-822.
6. Ye, B.; Akamatsu, M.; Shoelson, S. E.; Wolf, G.; Giorgetti-Peraldi, S.; Yan, X. J.; Roller, P. P.; Burke, T. R. *J. Med. Chem.* **1995**, *38*, 4270-4275.
7. Burke, T. R., Jr.; Ye, B.; Akamatsu, M.; Ford, H.; Yan, X. J.; Kole, H. K.; Wolf, G.; Shoelson, S. E.; Roller, P. P. *J. Med. Chem.* **1996**, *39*, 1021-1027.
8. Akamatsu, M.; Roller, P. P.; Chen, L.; Zhang, Z. Y.; Ye, B.; Burke, T. R., Jr. *Bioorg. Med. Chem.* **1997**, *5*, 157-163.

9. Akamatsu, M.; Ye, B.; Yan, X. J.; Kole, H. K.; Burke, T. R., Jr.; Roller, P. P. "Characterization of tyrosine-phosphate mimick containing tyrosine phosphatase inhibitory peptides."; 1995 Japan Peptide Symposium Proceedings, 1995, Osaka, Japan.
10. Bjorkling, F.; Boutelje, J.; Gatenbeck, S.; Hult, K.; Norin, T.; Szmulik, P. *Tetrahedron* **1985**, *41*, 1347-1352.
11. Luyten, M.; Muller, S.; Herzog, B.; Keese, R. *Helv. Chim. Acta* **1987**, *70*, 1250-1254.
12. Leonard, F.; Wajngurt, A.; Tshannen, W.; Block, F. B. *J. Med. Chem.* **1965**, *8*, 812-815.
13. Arnold, Z.; Larsen, P. O. *Acta Chem. Scand. B* **1977**, *31*, 826-828.
14. Jung, M. E.; Lazarova, T. I. *J. Org. Chem.* **1997**, *62*, 1553-1555.
15. Boger, D. L.; Yohannes, D. *J. Org. Chem.* **1987**, *52*, 5283-5286.
16. Burke, T. R., Jr.; Smyth, M. S.; Otaka, A.; Roller, P. P. *Tetrahedron Lett.* **1993**, *34*, 4125-4128.
17. Rzeszutarska, B.; Nadolska, B.; Tarnawski, J. *Liebigs Ann. Chem.* **1981**, 1294-1302.
18. Zhang, Z. Y.; Maclean, D.; Mcnamara, D. J.; Sawyer, T. K.; Dixon, J. E. *Biochemistry* **1994**, *33*, 2285-2290.
19. Burke, T. R., Jr.; Kole, H. K.; Roller, P. P. *Biochem. Biophys. Res. Commun.* **1994**, *204*, 129-134.
20. Chen, L.; Wu, L.; Otaka, A.; Smyth, M. S.; Roller, P. P.; Burke, T. R.; Denhertog, J.; Zhang, Z. Y. *Biochem. Biophys. Res. Commun.* **1995**, *216*, 976-984.
21. Rink, H. *Tetrahedron Lett.* **1987**, *28*, 3787-3790.
22. Garbay-Jaureguiberry, C.; McCort-Tranchepain, I.; Barbe, B.; Ficheux, D.; Roques, B. P. *Tetrahedron Assym.* **1992**, *3*, 637-650.
23. Gilmer, T.; Rodriquez, M.; Jordan, S.; Crosby, R.; Alligood, K.; Green, M.; Kimery, M.; Wagner, C.; Kinder, D.; Charifson, P.; Hassell, A. M.; Willard, D.; Luther, M.; Rusnak, D.; Sternbach, D. D.; Mehrotra, M.; Peel, M.; Shampine, L.; Davis, R.; Robbins, J.; Patel, I. R.; Kassel, D.; Burkhart, W.; Moyer, M.; Bradshaw, T.; Berman, J. *J. Biol. Chem.* **1994**, *269*, 31711-31719.
24. Waksman, G.; Shoelson, S. E.; Pant, N.; Cowburn, D.; Kuriyan, J. *Cell* **1993**, *72*, 779-790.
25. Note: For consistency with the literature, in which the X-ray structure of N-deacetyl **27** bound to PTP1B was reported,²⁶ modelling simulations on peptides **27**, **29** and **30** were conducted with these peptides lacking N-terminal acetylation.
26. Jia, Z.; Barford, D.; Flint, A. J.; Tonks, N. K. *Science* **1995**, *268*, 1754 - 1758.
27. Molecular Simulations, Inc., San Diego, CA.
28. Burke, T.R., Jr.; Zhang, Z. Y. *Peptide Science* (in press).
29. Brooks, C. L.; Karplus, M.; Pettitt, B. M. "Proteins: A theoretical perspective of dynamics, structure and thermodynamics" **1988**, Wiley, New York.
30. Kole, H. K.; Ye, B.; Akamatsu, M.; Yan, X.; Barford, D.; Roller, P. P.; Burke, T. R., Jr. *Biochem. Biophys. Res. Commun.* **1995**, *209*, 817-822.
31. Wavefunction Inc., Irvine, CA.
32. Chen, L.; Montserat, J.; Lawrence, D. S.; Zhang, Z. Y. *Biochemistry* **1996**, *35*, 9349-9354.
33. Zhang, Z. Y. *J. Biol. Chem.* **1995**, *270*, 11199-11204.
34. Wang, W.; Obeyesekere, N. U.; McMurry, J. S. *Tetrahedron Lett.* **1996**, *37*, 6661-6664.